Stem Cell Reports
Article

ISSCR

OPEN ACCESS

Mowat-Wilson syndrome factor ZEB2 controls early formation of human neural crest through BMP signaling modulation

Rebekah M. Charney,[1,3,*] Maneeshi S. Prasad,[1,3] Czarina Juan-Sing,[1] Lipsa J. Patel,[1] Jacqueline C. Hernandez,[1] Jie Wu,[2] and Martín I. García-Castro[1,*]

[1]Division of Biomedical Sciences, University of California, Riverside, Riverside, CA, USA
[2]Department of Biological Chemistry, University of California, Irvine, Irvine, CA, USA
[3]Present address: Department of Biochemistry, Jacobs School of Medicine and Biomedical Sciences, State University of New York at Buffalo, Buffalo, NY, USA
*Correspondence: rmcharney@gmail.com (R.M.C.), martin.garcia-castro@ucr.edu (M.I.G.-C.)
https://doi.org/10.1016/j.stemcr.2023.10.002

SUMMARY

Mowat-Wilson syndrome is caused by mutations in *ZEB2*, with patients exhibiting characteristics indicative of neural crest (NC) defects. We examined the contribution of ZEB2 to human NC formation using a model based on human embryonic stem cells. We found *ZEB2* to be one of the earliest factors expressed in prospective human NC, and knockdown revealed a role for ZEB2 in establishing the NC state while repressing pre-placodal and non-neural ectoderm genes. Examination of ZEB2 N-terminal mutant NC cells demonstrates its requirement for the repression of enhancers in the NC gene network and proper NC cell terminal differentiation into osteoblasts and peripheral neurons and neuroglia. This ZEB2 mutation causes early misexpression of BMP signaling ligands, which can be rescued by the attenuation of BMP. Our findings suggest that ZEB2 regulates early human NC specification by modulating proper BMP signaling and further elaborate the molecular defects underlying Mowat-Wilson syndrome.

INTRODUCTION

The neural crest (NC) is a multipotent cell population unique to vertebrates that migrates extensively and contributes to many cell types in the developing embryo (Douarin and Kalcheim, 1999). Although NC cells are associated with a large number of human health conditions, including cleft lip and cleft palate, rare syndromes, and cancers (Watt and Trainor, 2013; Charney et al., 2021), comparatively little is understood regarding the formation of human NC (hNC) cells. Mowat-Wilson syndrome (MWS) is a neurocristopathy caused by heterozygous mutations in *ZEB2* (ZFHX1B/SIP1) (Cacheux et al., 2001; Wakamatsu et al., 2001; Mowat et al., 1998). MWS patients exhibit a characteristic facial gestalt—which includes a high forehead, broad nasal bridge, posteriorly rotated ears with uplifted earlobes, hypertelorism, and an open mouth (Adam et al., 2006; Ivanovski et al., 2018)—and intellectual disability, and they frequently present with microcephaly, congenital heart defects, and Hirschsprung's disease, among other anomalies (Ivanovski et al., 2018). This phenotype is consistent with the role of ZEB2 as a major developmental regulator of both the neural and NC lineages.

ZEB2 is a multi-zinc finger transcriptional repressor that recognizes and binds to consensus E-box binding motifs (Verschueren et al., 1999) and can interact with the receptor-activated SMADs of the BMP and TGF-β pathways to inhibit the expression of downstream targets (Postigo, 2003; Verschueren et al., 1999). It is known for its role as a regulator of the epithelial-to-mesenchymal transition (EMT) in both embryonic development and cancer and functions extensively in the development of the central nervous system (Fardi et al., 2019; Vandewalle, 2005). However, its precise function in NC cell specification, formation, and differentiation, particularly during human development, is not well understood.

Recent advances in stem cell technologies have allowed for the investigation of hNC cell formation and differentiation *in vitro* (Lee et al., 2010; Menendez et al., 2011; Leung et al., 2016; Gomez et al., 2019; Hackland et al., 2019). In this study, we examined the role of ZEB2 in early hNC development using a human embryonic stem cell (hESC)-based model of cranial hNC induced through two days of exogenous Wnt signaling (Gomez et al., 2019). This model is consistent with the requirement for Wnt, BMP, and FGF signals during NC induction, and a detailed assessment of molecular markers reveals time points similar to developmental stages seen *in vivo* such as a neural plate border (NPB)-like and NC state characterized by expression of all known markers (Leung et al., 2016; Gomez et al., 2019; Prasad et al., 2020a).

Using this model, we previously identified the early expression of *ZEB2* and suggested it was among the earliest factors responsive to Wnt signaling during NC formation (Leung et al., 2016). Here, we reveal the gene network regulated by ZEB2 during hNC cell induction. We find that *ZEB2* is rapidly activated and continuously expressed during hNC induction, and this expression is consistent with early *Zeb2* expression in the chick embryo. Knockdown of ZEB2 results in significant changes in the expression of genes associated with the NC cell state and the EMT, as

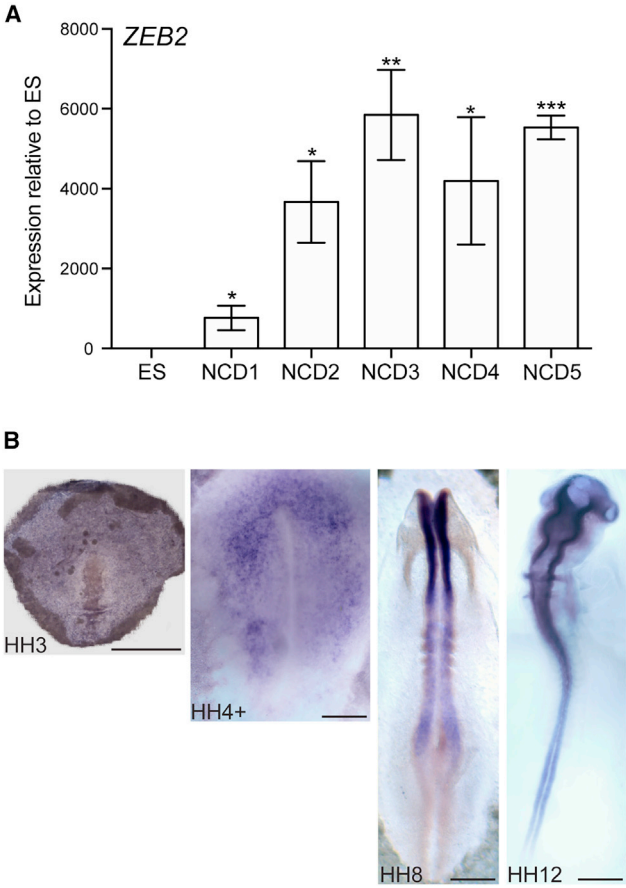

Figure 1. Expression of *ZEB2* in human neural crest and early chick embryos

(A) qRT-PCR analysis of *ZEB2* expression during hNC cell induction. Data from 3 independent experiments with SEM. *p ≤ 0.05, **p ≤ 0.01, and ***p ≤ 0.001.

(B) Whole-mount *in situ* hybridization revealing *Zeb2* expression in the early chick embryo. A representative image is shown. Scale bars, 1 mm.

well as the up-regulation of genes associated with the preplacodal and non-neural ectoderm. To gain insight into the repressive mechanisms of ZEB2, we examined ZEB2 N-terminal mutant hNC cells and their derivatives. Mutant ZEB2 lacking the nucleosome remodeling and deacetylase (NuRD) complex interacting domain loses the ability to interact with HDAC1, and chromatin accessibility analysis revealed derepressed putative enhancers during hNC induction. ZEB2 mutant hNC cells further displayed a reduced ability to terminally differentiate into osteoblasts, peripheral neurons, and neuroglia. Finally, we reveal that the gene expression changes resulting from this mutation can be rescued through the inhibition of BMP signaling, indicating that ZEB2 plays a role in modulating the proper levels of BMP signaling required for hNC formation. This work sheds light on the role of ZEB2 during hNC formation and provides a basis for further studies exploring the mechanisms underlying MWS.

RESULTS

ZEB2 is rapidly expressed during NC induction

Zeb2 transcripts are expressed in the neural epithelium and in the prospective and migrating NC cells in mouse, chick, and frog (van Grunsven et al., 2000; Putte et al., 2003; Rogers et al., 2013). Using qRT-PCR, in our model of cranial hNC (Gomez et al., 2019) we identified *ZEB2* expression at day 1 of hNC induction and a continued increase in expression over the course of 5 days (Figure 1A). RNA sequencing (RNA-seq) analysis confirms this expression pattern, and further reveals the onset of *ZEB2* expression as early as 12 h (data not shown). These findings confirm and expand upon our previously reported hNC expression patterns (Leung et al., 2016) and indicate that *ZEB2* is rapidly activated and maintained throughout hNC formation.

In the amniote chick embryo, *Zeb2* has been observed in the prospective neural plate (Hamburger-Hamilton stage 4 [HH4] and HH5), the NPB (HH7), and in the migrating NC cells (HH9–HH13) (Acloque et al., 2017; Rogers et al., 2013). Similar to the rapid expression of *ZEB2* in hNC cells, using *in situ* hybridization we observed *Zeb2* expression throughout the entire epiblast of the chick HH3 gastrula embryo (Figure 1B), prior to the expression of earliest NC specification marker *Pax7* (Basch et al., 2006). Consistent with previous reports, at HH4+, *Zeb2* becomes restricted to the prospective neural plate and NC, and by HH8 *Zeb2* expression is observed in the neural folds (Figure 1B). In the HH12 embryo, *Zeb2* expressing cells are observed in the neural tube and in streams of migrating NC (Figure 1B). Together, these findings indicate that expression of *ZEB2* transcripts begins at very early stages of amniote NC specification and is maintained throughout stages of NC formation.

ZEB2 regulates the expression of NPB and NC genes during hNC induction

To address the role of ZEB2 during early hNC induction, we used a small interfering RNA (siRNA)-based knockdown of ZEB2 in our hNC model (Figure 2A). Knockdown assessed at day 2 of hNC induction revealed an ~80% reduction in ZEB2 protein expression (Figure S1A) and a ~50% reduction in *ZEB2* transcripts (Figure S1B). Using qRT-PCR, we observed an increase in NPB gene expression at day 3 and a decrease of NC-specifier gene expression at day 5 (Figure S1C). Consistent with previous reports (Putte et al., 2003; Rogers et al., 2013; Vandewalle, 2005), *CDH1* expression was increased.

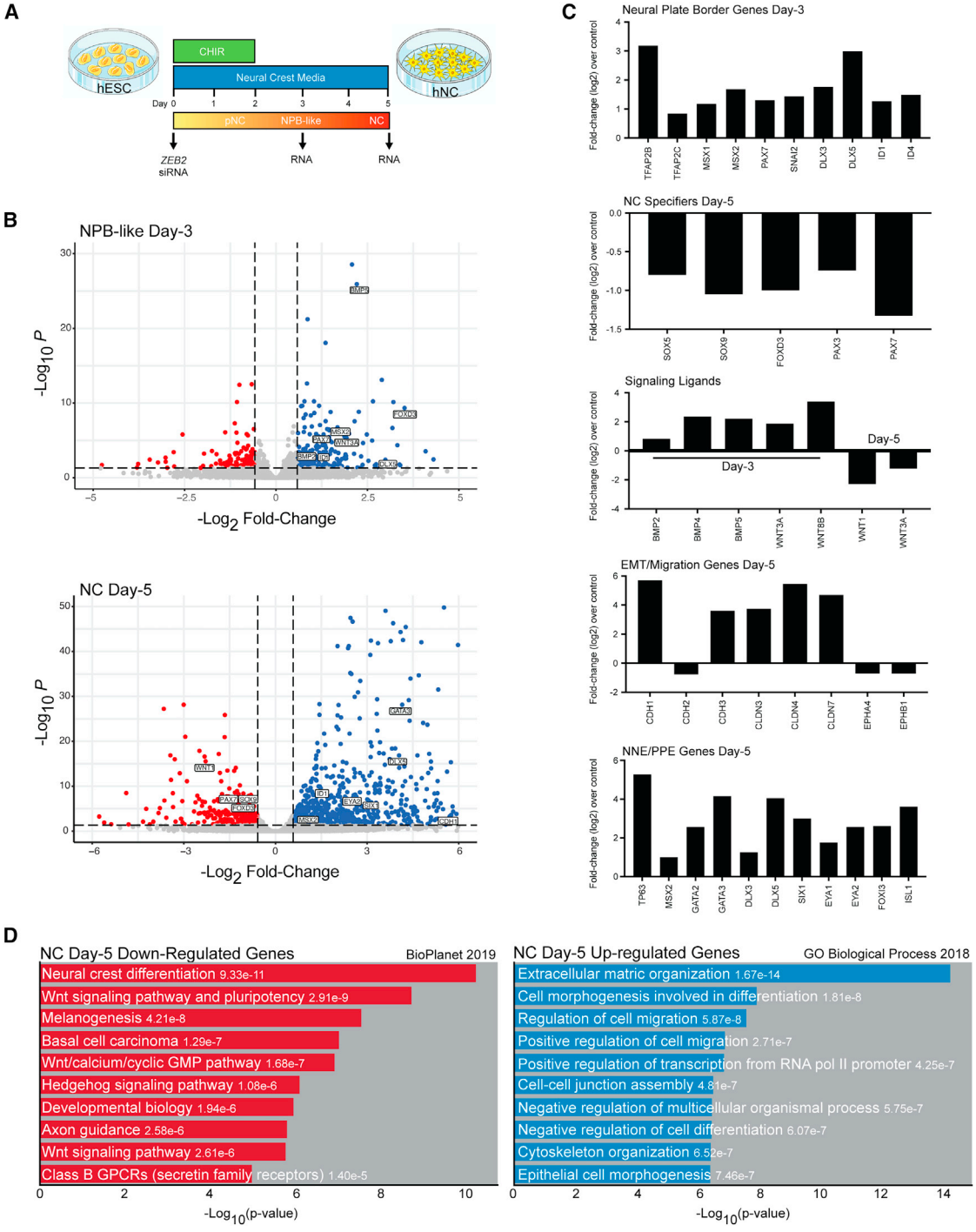

Figure 2. Knockdown of ZEB2 causes misregulation of NC, non-neural, and pre-placodal ectodermal genes

(A) Schematic of siRNA knockdown.

(B) Volcano plots representing RNA-seq differentially expressed genes measured between non-targeting control and ZEB2 knockdown at day 3 and day 5. Blue, fold change $\geq$ 1.5 and adjusted p $\leq$ 0.05; red, fold change ≤ -1.5 and adjusted p $\leq$ 0.05; gray, $-1.5 <$ fold change < 1.5 and/or adjusted $p > 0.05$.

(C) Gene expression changes of select gene modules measured using RNA-seq following ZEB2 knockdown.

(D) Gene enrichment analysis of hNC day 5 differentially expressed genes.

To examine the global gene expression changes, we performed RNA-seq at hNC day 3 and day 5 following ZEB2 knockdown and compared it with the stage-matched non-targeting control (NTC) (Figure 2A). At day 3, 341 genes were significantly differentially expressed, with 218 genes up-regulated and 123 genes down-regulated (Figure 2B, top; Table S1). Pathway enrichment analysis revealed NC differentiation as the top enriched pathway in up-regulated genes, with terms associated with TGF-β signaling also enriched (Figure S1D). We observed the up-regulation of NPB genes (e.g., *PAX7*, *MSX1*/2, *DLX5*), NC specifiers (e.g., *FOXD3*, *SOX9*, *SNAI2*, *ID* factors), and ligands and signaling modulators associated with the BMP and Wnt signaling pathways (Figures 2B and 2C). Of note, the NPB/NC-specifier gene *ZIC1* was among the 123 down-regulated genes following ZEB2 knockdown at day 3.

At day 5, the knockdown of ZEB2 resulted in significant expression changes of 1,105 genes, with 802 genes up-regulated and 303 genes down-regulated (Figure 2B, bottom; Table S1). Although NPB and NC-specifier genes were up-regulated at day 3, NPB and NC-specifier genes were down-regulated at day 5 (Figures 2B and 2C) – indicating a failure of proper NC cell formation. Components of the Wnt signaling pathway including ligands *WNT1*, *WNT3A*, and *WNT7B*, along with the Wnt effector *SP5*, were also down-regulated at day 5. Consistent with this, pathway enrichment analysis revealed NC differentiation and Wnt signaling pathway at the top enriched terms among the day 5 down-regulated genes (Figure 2D). Genes up-regulated at day 5 were enriched for terms related to the regulation of the extracellular matrix (Figure 2D), and we observed changes in the expression of *CDH1*, *CDH2*, and *CDH3*, as well as claudins and Eph receptors (Figure 2C). Finally, at day 5, we observed the up-regulation of pre-placodal and non-neural ectoderm markers (Figures 2B and 2C). The day 5 decrease of NC gene expression together with the increase in expression of pre-placodal and non-neural ectoderm markers suggests a requirement for ZEB2 in ectodermal cell fate patterning. Taken together, these findings suggest a role for ZEB2 in the proper formation of hNC cells where the misregulation of NPB factors and signaling molecules at day 3 results in impaired formation of NC cells at day 5.

The ZEB2 N terminus is required for hNC cell formation and differentiation

ZEB2 is a transcriptional repressor which recruits the NuRD complex through an N-terminal interaction domain (Verstappen et al., 2008) (Figure 3A). The NuRD complex promotes chromatin repression through the recruitment of HDAC1/2 and ATP-dependent nucleosome remodeling through CHD3/4 (Ahringer, 2000). Importantly, frameshift causing mutations in the ZEB2 N terminus have been reported in MWS patients (Ivanovski et al., 2018). To gain insight into the requirement of the ZEB2 N terminus during hNC cell formation, we made use of CRISPR-Cas9 genome editing to generate an hESC line containing a homozygous N-terminal *ZEB2* mutation (ZEB2 N-mutant) (Figure 3A). In this cell line, a frameshift causing mutation in exon 3 is predicted to result in the use of an alternative start codon in exon 4 with the resulting truncated ZEB2 protein lacking the first 112 amino acids (Figures 3A and S2A). This ZEB2 N-mutant hESC line retains normal expression of pluripotency factors when cultured under non-differentiating conditions as assessed by immunofluorescence staining for POU5F1 and SOX2, and RNA-seq transcriptomic analysis (Figures S2B and S2C). Western blot analysis confirmed the expression of truncated ZEB2 N-mutant compared with wild-type (WT) ZEB2 in day 5 hNC cells, with the expression level of ZEB2 N-mutant equal to full-length ZEB2 in the isogenic WT cells (Figures 3B and S2D). Furthermore, endogenous co-immunoprecipitation revealed the loss of HDAC1 interaction in the ZEB2 N-mutant compared with WT in day 5 hNC cells (Figure 3C). This finding suggests that the NuRD-interacting domain is required for ZEB2's association with HDAC1 during hNC cell formation.

We next used RNA-seq to assess the transcriptional changes during NC induction resulting from the loss of the N terminus (Figures 3D and S3A; Table S2). At day 3, we identified 552 differentially enriched genes in ZEB2 mutant NC compared with WT, including the up-regulation of genes encoding NPB markers, NC specifiers, and BMP ligands and regulators. Pathway enrichment analysis revealed the significant enrichment of terms associated with NC cell differentiation (Figure S3B). At day 5, 865 genes exhibited significant expression changes, revealing the down-regulation of NC specifiers and Wnt signaling ligands, and the up-regulation of genes associated with extracellular matrix organization and the non-neural and pre-placodal ectoderm fates (Figure S3C). Finally, genes associated with NC terminal derivatives, including Schwann cell markers *GAP43* and *S100B*, osteoblast marker *BGLAP*, and peripheral neuron markers *POU4F1* and *TAC1* were also differentially enriched (Table S2).

MWS patients exhibit craniofacial and neurological anomalies that appear associated with the NC lineage. Hence, we assessed the role of ZEB2 in the formation of NC derivatives including craniofacial bone and peripheral neurons and glia. Osteoblast differentiation was severely affected in ZEB2 N-mutant hNC cells compared with WT as observed through calcification after a 30-day differentiation (Figure 3E). We further identified an approximately 50% decrease in cell proliferation in the ZEB2 mutant osteoblasts using BrdU staining (Figure S3D). Next, we assessed the effect of ZEB2 N-mutant on Schwann cell

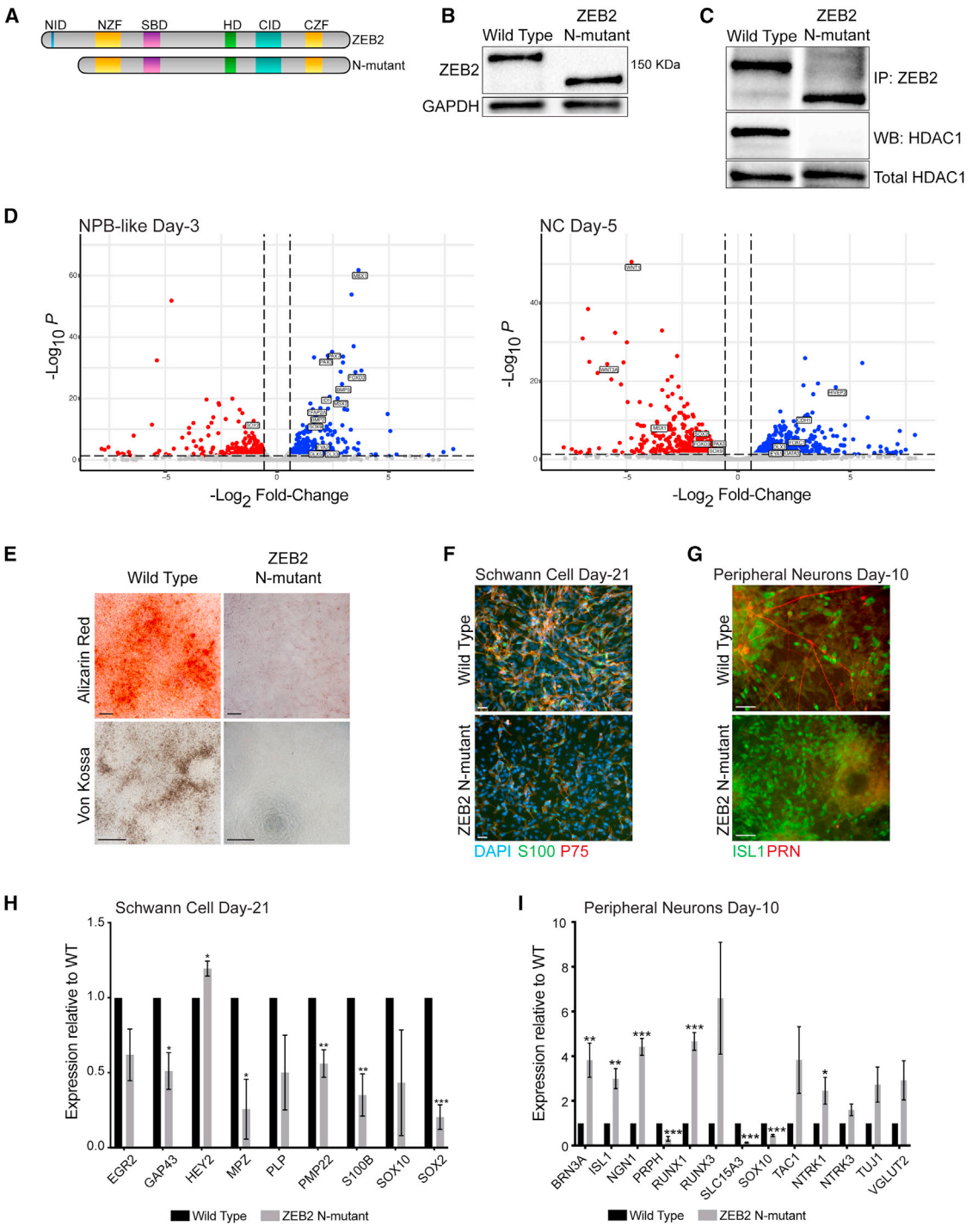

Figure 3. N-terminal ZEB2 truncation inhibits neural crest cell formation and differentiation

(A) Schematic of the ZEB2 N-terminal mutant compared with WT ZEB2.

(B) Western blot analysis of ZEB2 protein from day 5 WT and ZEB2 N-mutant hNC cells.

(C) Co-immunoprecipitation of ZEB2 and HDAC1 in day 5 hNC cells. Total HDAC1 protein probed from input collected prior to immunoprecipitation.

(legend continued on next page)

differentiation. Through immunofluorescence and qRT-PCR, we observed a marked decrease in Schwann cell markers at the end of a 21-day differentiation of Schwann cells from ZEB2 N-mutant hNC cells (Figures 3F and 3H). We also observed the up-regulation of *HEY2*, a negative regulator of Schwann cell maturation and a putative target of ZEB2 (Quintes et al., 2016) (Figure 3H).

Finally, we examined peripheral neural differentiation in the ZEB2 N-mutant background at day 10 (Figures 3G and 3I) and day 26 (Figures S3E and S3F). Peripheral neural markers were significantly misregulated at both time points. At day 10, markers including *BRN3A*, *ISL1*, *NGN1*, *RUNX1*, and *NTRK1* were up-regulated and *PRPH*, *SLC15A3*, and *SOX10* were down-regulated, with the continued up-regulation of *BRN3A* and *NGN1* and down-regulation of *PRPH*, at day 26. Interestingly, at day 26, *NTRK1* was down-regulated (Figure S3E). Immunofluorescence further validated the changes in PRPH and ISL1 protein expression as well as reduced proliferation and axonal projections in the ZEB2 mutant cells compared with WT (Figure S3F). Together, these findings indicate that the ZEB2 N terminus is required for its proper function during hNC cell induction and suggest a misregulation in the NC gene regulatory network in MWS causing ZEB2 truncations.

ZEB2 N-mutant alters hNC chromatin accessibility

As mutant ZEB2 loses interaction with HDAC1 (Figure 3C), we hypothesized that it is unable to facilitate repression of enhancers in the NC gene regulatory network. To explore changes in the epigenetic landscape, we performed an assay for transposase-accessible chromatin with sequencing (ATAC-seq) on WT and ZEB2 mutant day 3 and day 5 hNC. Correlation analysis of the ATAC-seq reads in each condition revealed that the data clusters on the basis of NC stage, not sample type (Figure S4). We identified differentially enriched peaks at each stage, including 691 peaks that were shared between day 3 and day 5 (Figure 4A; Table S3). Our finding that most differentially enriched peaks were derepressed supports the role of the NuRD complex and the canonical function of ZEB2 as a repressor.

We associated, within 500 kb, the differentially enriched regions at each day with 2,114 unique genes at day 3 and 8,206 unique genes at day 5 (Table S3), which include genes associated with NC, NC derivatives, non-neural ectoderm, and pre-placodal ectoderm. For example, at day 3, we observed increased regions of accessibility associated with *BMP2* and *BMP5* (Figure 4B), consistent with the day 3 up-regulation of these transcripts. We also observed peaks at both day 3 and day 5 that were differentially enriched in a dynamic fashion, including peaks associated with *PAX7* and the pre-placodal markers *EYA1* and *EYA2* (Figure 4B). Finally, we identified differentially enriched peaks associated with NC cell derivatives, including *GAP43* (Schwann cells), *MITF* (melanocytes), *COL2A1* (chondrocytes), *ALPL* (osteoblasts), and *POU4F1* (peripheral neurons) (Figure S5).

To explore the temporal dynamics of the differentially enriched peaks, we generated heatmaps representing the ATAC-seq signal over the day 3 and day 5 differentially enriched peaks, which were clustered using k-means (Figure 4C; Table S3). At both time points, we identified clusters representing stage-specific derepression (e.g., day 3 clusters 1, 2, and 5 and day 5 clusters 3, 4, and 7) and repression (day 3 cluster 3 and day 5 clusters 5 and 8), as well as clusters containing prematurely derepressed peaks (day 3 clusters 1 and 4). This analysis suggests that ZEB2's regulation of chromatin accessibility is highly stage specific.

These observed temporal dynamics of enhancer accessibility suggest that perhaps ZEB2-regulated peaks are bound by different transcription factors at different times during NC formation. To examine the putative proteins that bind to the differentially enriched regions, we performed *de novo* motif analysis on the DNA sequences under the differentially enriched peaks (Figure 4D; Table S4). Motif analysis was carried out on ZEB2 N-mutant increased peaks at day 3 and day 5 and day 5 ZEB2 N-mutant decreased peaks. At both time points, we identified the enrichment of ZEB2 and TFAP2 motifs underneath the ATAC-seq

(D) Volcano plots representing RNA-seq differentially expressed genes between WT and ZEB2 N-mutant hNC at day 3 and day 5. Blue, fold change $\geq$ 1.5 and adjusted p $\leq$ 0.05; red, fold change ≤ -1.5 and adjusted p $\leq$ 0.05; gray, -1.5 < fold change < 1.5 and/or adjusted p > 0.05.

(E) Osteoblasts differentiated from day 5 WT and ZEB2 N-mutant hNC cells. Calcification was assessed after 30 days of culture using Alizarin red (scale bars, 100 μm) and Von Kossa staining (scale bars, 500 μm). A representative image is shown.

(F) S100B and P75NTR immunostaining of day 21 Schwann cells differentiated from WT and ZEB2 N-mutant NC cells. A representative image is shown. Scale bars, 50 μm.

(G) ISL1 and PRPH immunostaining of day 10 peripheral neurons differentiated from WT and ZEB2 mutant NC cells. A representative image is shown. Scale bars, 50 μm.

(H) qRT-PCR analysis of Schwann cell markers at day 21. Data from 3 independent experiments with SEM. *p $\leq$ 0.05, **p $\leq$ 0.01, and ***p $\leq$ 0.001.

(I) qRT-PCR analysis of markers of peripheral neurons at day 10. Data from 4 independent experiments with SEM. *p $\leq$ 0.05, **p $\leq$ 0.01, and ***p $\leq$ 0.001.

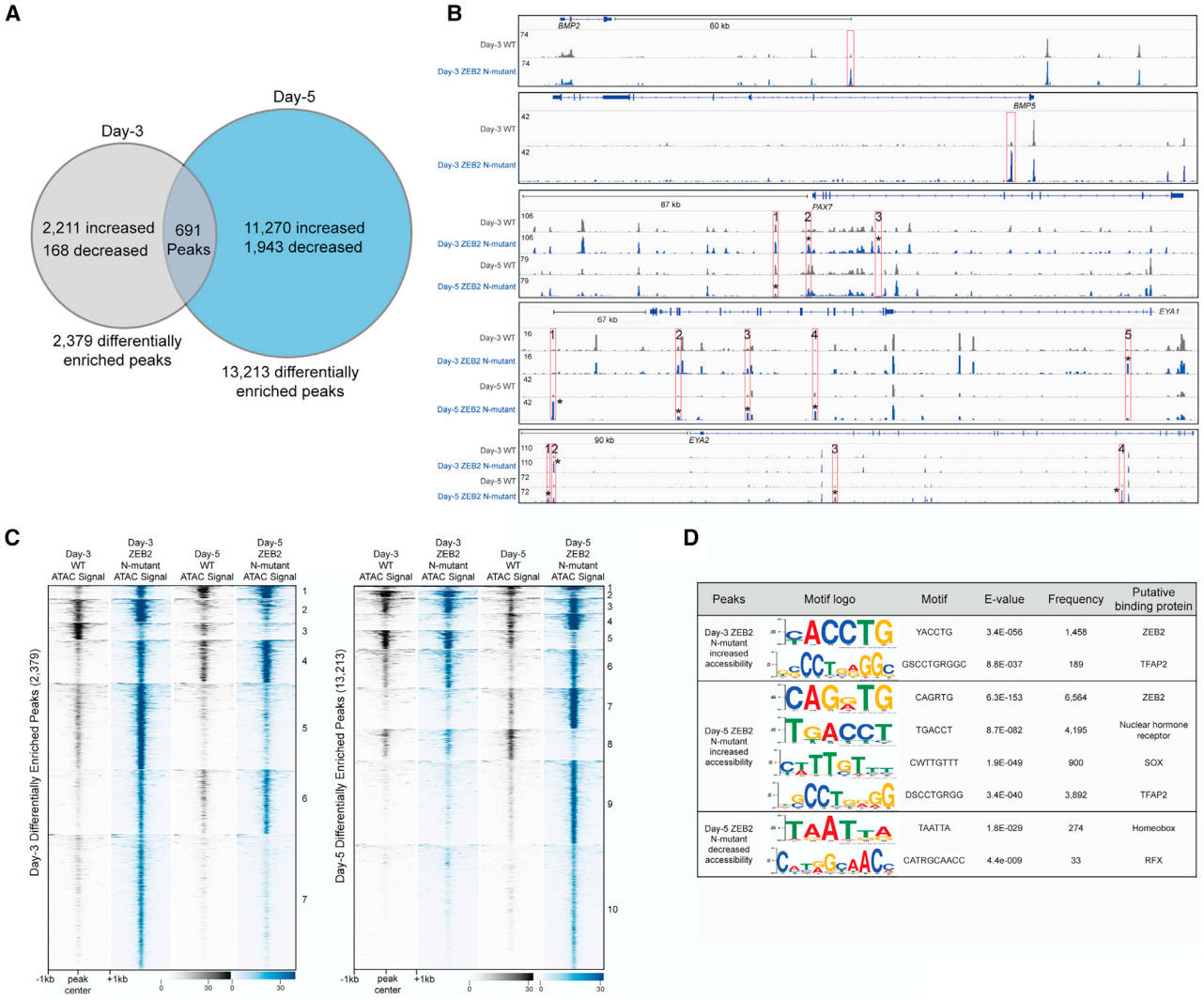

Figure 4. ZEB2 truncation derepresses putative enhancers in the neural crest gene regulatory network

(A) ATAC-seq peaks differentially enriched between WT and ZEB2 N-mutant hNC cells.

(B) Integrated Genome Viewer tracks displaying ATAC-seq signal associated with select genes. Differentially enriched peaks are marked in red.

(C) Heatmaps displaying day 3 (left) and day 5 (right) ATAC-seq signal centered on the differentially enriched peaks at the indicated stage. Heatmaps were k-means clustered with 7 clusters for day 3 and 10 clusters for day 5.

(D) *De novo* motif analysis of genomic sequences (150 bp) centered on the summits of differentially enriched ATAC-seq peaks. Top motifs are shown in the table and full motif output is reported in Table S5.

increased peaks. At day 5, binding motifs for the nuclear hormone receptor superfamily and the SOX family were found within the increased accessibility peaks, while enriched motifs found under the ZEB2 N-mutant decreased accessibility peaks include those for homeobox containing transcription factors and RFX transcription factors. Our *de novo* motif analysis did not identify the ZEB2-binding motif as enriched under the peaks with decreased ATAC-seq accessibility, suggesting that the observed decrease in gene expression, including the down-regulation of NC genes, in most cases is likely to be an indirect result of perturbations in the gene regulatory network.

ZEB2 N terminus is required to modulate levels of BMP signaling during hNC cell formation

Transcriptomic analysis of ZEB2 knockdown and ZEB2 N-mutant hNC both revealed the up-regulation of BMP ligands, regulators, and targets, particularly at the NPB-like state day 3 (Figure 5A). Studies in animal models suggest that attenuated levels of BMP signaling is required to

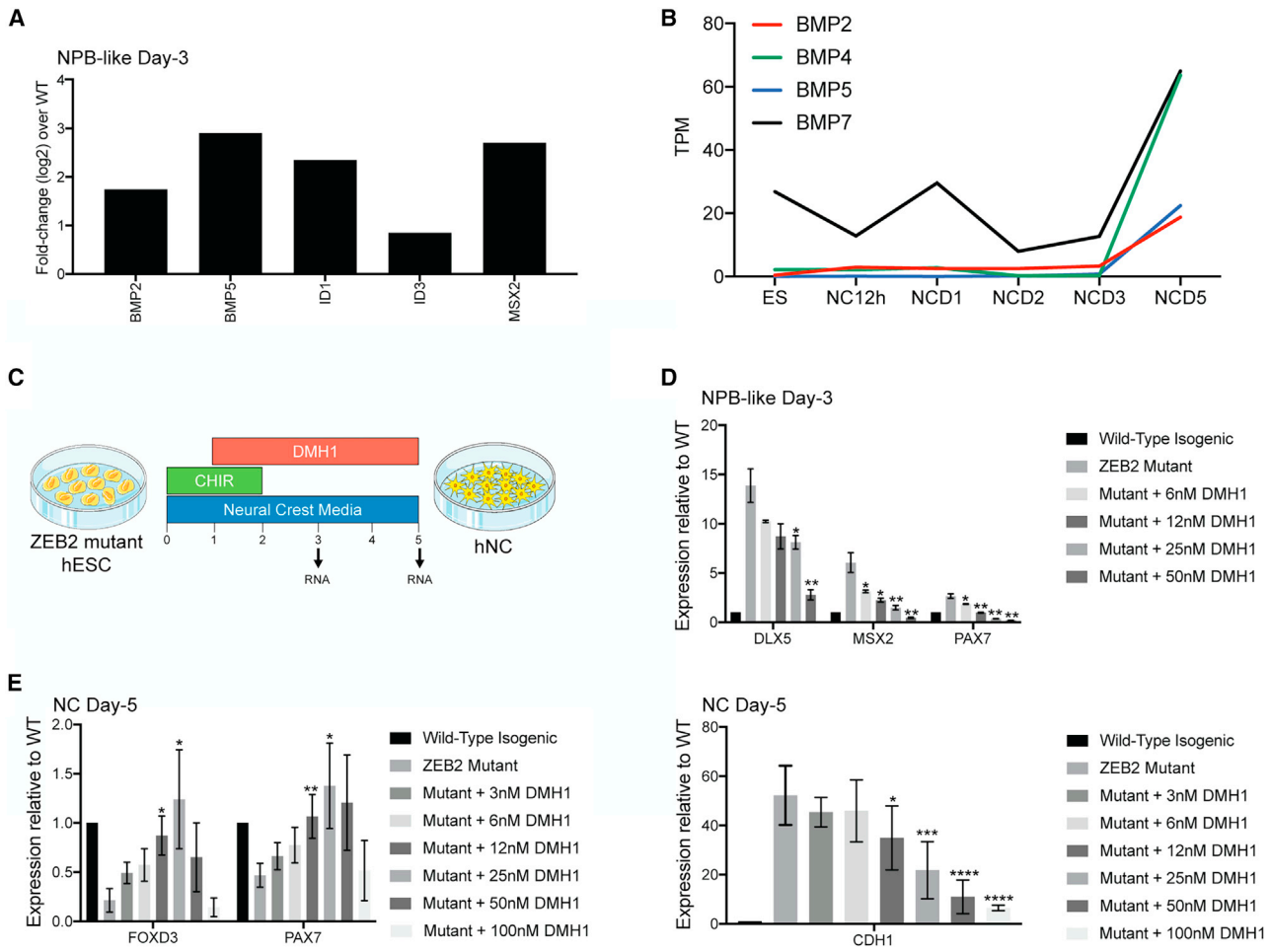

Figure 5. Inhibition of BMP signaling during neural crest induction rescues the ZEB2 truncation phenotype

(A) Gene expression changes of BMP ligands and BMP-responsive genes at day 3 observed in ZEB2 mutant NC RNA-seq. See also Figure 3D.

(B) Expression levels of BMP ligands during hNC cell induction. Mean of 2 independent experiments.

(C) Schematic of BMP inhibition experiment. Indicated concentrations of DMH1 was added to the hNC media beginning at day 1.

(D) qRT-PCR analysis of *DLX5*, *MSX2*, and *PAX7* under isogenic WT, ZEB2 mutant, and DMH1 rescue conditions at day 3. Data from 3 independent experiments with SEM. p values calculated to ZEB2 mutant: *p $\leq$ 0.1 and **p $\leq$ 0.05.

(E) qRT-PCR analysis of *FOXD3*, *PAX7* (left), and *CDH1* (right) at day 5. Data from 3 independent experiments with SEM. p values calculated to ZEB2 mutant: *p $\leq$ 0.1, **p $\leq$ 0.05, ***p $\leq$ 0.01, and ****p $\leq$ 0.001.

properly induce NC at the NPB, which is subsequently followed by a reactivation of BMP signaling to promote the expression of NC specifiers (LaBonne and Bronner-Fraser, 1998; Marchant et al., 1998; Steventon et al., 2009). Interestingly, transcriptomic analysis over the time course of hNC induction revealed low expression of BMP ligands through day 3, increasing at day 5 (Figure 5B). ZEB2 is a known Smad binding partner with the ability to inhibit BMP signaling (Postigo, 2003; Verschueren et al., 1999). Although the role of ZEB2 has been well documented to inhibit BMP signaling during neural development (Nitta et al., 2004), its role in modulating BMP signaling during NC cell formation is unknown. To address this, we used the small molecule BMP inhibitor DMH1 to rescue the gene expression changes observed in ZEB2 N-mutant hNC (Figure 5C). Through careful titration, we found that concentrations of less than 100 nM were sufficient to rescue the gene expression changes observed in the ZEB2 N-mutant hNC at both day 3 and day 5 (Figures 5D and 5E). Gene expression rescue was observed in a dose dependent manner. Although 12 nM DMH1 is significant to rescue the NPB/NC markers assayed, we noted that higher doses (50–100 nM) were needed to rescue the non-neural ectoderm markers *DLX5* (day 3) and *CDH1* (day 5). Together, these findings support the notion that the premature up-regulation of BMP signaling is a hallmark of ZEB2 loss of function and that the modulation of BMP signaling during early hNC is a critical function of ZEB2.

DISCUSSION

MWS is a rare disorder caused by heterozygous mutations in *ZEB2* and marked by characteristic facial features, intellectual defects, and other anomalies. Our study interrogated the role of the ZEB2 repressor during hNC cell formation and suggests a role for ZEB2 in promoting the NC lineage and repressing the non-neural and pre-placodal ectoderm fates. Furthermore, our work using an N-terminal mutant of ZEB2 reveals the importance of the NuRD-interacting domain in ZEB2 regulation of NC cell development and suggests that ZEB2 functions in part to modulate the proper levels of BMP signaling during prospective NC stages.

We identified *ZEB2* expression starting at 12 h post-induction of hNC from hESCs and significantly increasing at day 1 and day 2 prior to the expression of NPB genes at day 3. In agreement with this, we observed *Zeb2* transcripts at stage HH3 of chick epiblast. Our findings indicate that *Zeb2* is expressed broadly in the upper layer of the gastrulating chick embryo including the territory shown to correspond to specified NC (Basch et al., 2006; Prasad et al., 2020b) and precedes expression of *Pax7* in the NPB. This is consistent with the early gastrula stage expression of *zeb2* in *Xenopus*, with transcripts first detectable in NF at stage 10 of early gastrula (van Grunsven et al., 2000). However, the regulatory network governing *ZEB2* expression in the early chick gastrula and its later modulation and restriction to the prospective neural plate and NPB remain unknown and should be the focus of future studies.

We explored the function of ZEB2 in hNC cell induction through both siRNA-mediated knockdown of ZEB2 during hNC induction and the generation of a hESC line containing an N-terminal ZEB2 mutant which lacks the repressive NuRD-interacting domain. Consistent with the role of ZEB2 as a EMT regulator (Comijn et al., 2001; Vandewalle, 2005) during development (DaSilva-Arnold et al., 2018; Kerosuo and Bronner-Fraser, 2012; Putte et al., 2003; 2007; Rogers et al., 2013; van den Berghe et al., 2013) and invasive cancer (Rosivatz et al., 2002; Elloul et al., 2005; Imamichi et al., 2007; Xia et al., 2010), the loss of ZEB2 in hNC resulted in changes in the expression of genes associated with EMT, such as cadherins. In addition, ZEB2 has been implicated in lineage specification (Chng et al., 2010; Strykjewska et al., 2016) and cell differentiation including corticogenesis (Seuntjens et al., 2009) and melanogenesis (Denecker et al., 2014), among others. We find that ZEB2 is required for the proper expression of NPB and NC-specifier genes, as well as WNT and BMP signaling pathway components. We further observed the up-regulation of pre-placodal and non-neural ectoderm genes at both day 3 and day 5 upon loss of ZEB2 expression. These findings suggest a model whereby ZEB2 is required early to promote proper NC specification and inhibition of the pre-placodal and non-neural ectoderm fates. Consistent with this, a lack of boundary between the neural and non-neural ectoderm has been observed in ZEB2-null mice (Putte et al., 2003).

We observed a global increase in DNA accessibility in ZEB2 N-mutant hNC, including differentially enriched peaks within or nearby NPB, NC, and PPE genes. This suggests that the loss of functional ZEB2 relieves repression of nearby putative enhancers. Importantly, motif analysis on the DNA sequence under the differentially enriched peaks revealed the enrichment of the ZEB2-binding motif under the regions of increased accessibility, suggesting that many of these regions are likely to be directly bound and repressed by ZEB2 via the NuRD complex. The generation of ZEB2 occupancy maps during hNC induction will be important to confirm ZEB2 binding to putative enhancers. Our motif analysis also revealed the enrichment of additional motifs including the pioneer factor TFAP2, which functions during NPB and NC cell specification (Rothstein and Simoes-Costa, 2019). This raises the intriguing possibility that TFAP2A pioneers ZEB2-modulated enhancers during hNC cell specification, and future analysis of TFAP2 occupancy of ZEB2-regulated regions will be necessary.

ZEB2 is known to modulate TGF-β signaling through interactions with receptor-activated Smads (Nitta et al., 2004; Postigo, 2003; Verschueren et al., 1999), as well as regulate BMP4 through direct enhancer binding (van Grunsven et al., 2007). Our finding that that suppression of BMP signaling using a small molecule inhibitor can rescue the ZEB2 mutant NC phenotype suggests that a major function of ZEB2 during early NC specification is to modulate the appropriate levels of BMP signaling. This finding, together with our transcriptomic and epigenetic analyses, leads us to speculate that ZEB2 regulates the expression of at least *BMP2* and *BMP5* during early hNC specification. Importantly, the misregulation of BMP signaling during the prospective NC stage would suggest a mechanism for our observation of increased PPE/NNE gene expression, as these factors respond to increased levels of BMP signaling (Saint-Jeannet and Moody, 2014). Although the SMAD binding motif was not identified as enriched in our *de novo* motif analysis, a targeted scan for the 5 bp GC motif (Martin-Malpartida et al., 2017) revealed an approximately 70% co-occurrence between the ZEB2 and SMAD motifs at both day 3 and day 5. It remains to be seen how ZEB2 interacts with R-SMADs in the downstream regulation of BMP signaling. Importantly, the derepression of putative enhancers near NPB genes in ZEB2 mutant cells, coupled with the day 3 increase in gene expression, suggests that ZEB2 is involved in the direct repression of these genes. It will be crucial to investigate whether R-SMADs are also

involved in target gene regulation through these enhancers.

Most ZEB2 mutations in MWS patients identified to date are nonsense or frameshift mutations which are generally expected to result in the nonsense-mediated decay of transcripts or in non-functional protein products. As awareness of the syndrome has increased, however, genotypes including missense, in-frame deletions, and splice-site mutations have been identified (Ivanovski et al., 2018), and the potential role of gain-of-function or dominant-negative mutations has been suggested (Heinritz et al., 2006). Given the variable clinical manifestations of MWS, it is critical to assess the functional effects of ZEB2 mutations. Here, we examined the NC defects arising from the loss of the ZEB2 N terminus, which includes the NuRD-interacting domain. Mutations affecting the NuRD-interacting domain have been described in MWS patients (Ivanovski et al., 2018; Zweier et al., 2006). Although these patients were reported to have a mild clinical phenotype, Zweier et al. noted the presence of the characteristic MWS facial features, suggesting that the N terminus might be important for the cranial NC cell lineage. Our analysis supports the requirement for the N terminus during hNC cell formation, as ZEB2 N-mutant NC cells displayed defects in osteoblast formation. This is in line with the NC-specific ablation of ZEB2 in mice, which demonstrated incomplete bone ossification (Putte et al., 2007). Although bone ossification has not been thoroughly studied in MWS patients, delayed bone age has been reported in a subset of patients (Ivanovski et al., 2018). We note that our results might represent a stronger osteoblast phenotype because of the homozygous ZEB2 mutation in our hESC line, compared with the heterozygous mutations observed in MWS patients, and future interrogation of heterozygous ZEB2 mutant hNC cells will be important. Furthermore, craniofacial bone is also derived from the mesoderm. Although not a focus of this study, it is interesting to note that the mesoderm-specific loss of ZEB2 results in craniofacial and dental defects in mice (Teraishi et al., 2017). Detailed investigations into the role of ZEB2 in both NC and mesoderm-derived craniofacial bone is warranted.

MWS patients have been reported to experience an under-reaction to pain (Evans et al., 2012), and ZEB2 has been shown to play a role in the formation of sensory dorsal root ganglia neurons in mice (Pradier et al., 2013; Ohayon et al., 2015). Our results indicate significant transcriptional changes in peripheral neurons derived from ZEB2 mutant hNC. ZEB2 has also been implicated in promoting Schwann cell differentiation, in particular by repressing inhibitors of differentiation (Quintes et al., 2016; Wu et al., 2016). Differentiation of our ZEB2 N-mutant NC cells into Schwann cells revealed a decrease in markers of Schwann cell precursors and myelination, and furthered revealed an increase in the expression of the Notch effector and Schwann cell differentiation inhibitor *HEY2*. The importance of ZEB2's NuRD-interacting domain has been reported in Schwann cell differentiation (Wu et al., 2016). We also observed the misregulation of *SOX2* expression in the Schwann cell lineage, which could be further attributed to the decreased expression of *SOX2* in ZEB2 mutant NC cells.

Our findings suggest that ZEB2 plays an early role in hNC specification by modulating BMP signaling to repress preplacodal and non-neural ectodermal cell fates and promote the NC lineage. We find that truncated ZEB2 fails to repress putative enhancers during NC cell formation and leads to NC differentiation defects, providing a better understanding of the mechanisms underscoring the MWS phenotype.

EXPERIMENTAL PROCEDURES

Resource availability

Corresponding author

Requests should be directed to Rebekah Charney (rmcharney@gmail.com).

Materials availability

All unique reagents generated in this study are available with a completed Materials Transfer Agreement.

Data and code availability

All high-throughput sequencing data reported in this paper have been deposited in the database of Genotypes and Phenotypes (dbGaP: phs002701.v1.p1).

hESC culture

H1 hESCs (WA01; WiCell Institute) of passages 24–35 were maintained on plastic surfaces coated with Matrigel (Corning) in mTeSR1 (STEMCELL Technologies). Cultures were passaged every 4–5 days using Versene (Gibco) when approximately 80% confluency was reached. Cells were routinely tested for mycoplasma contamination using Lonza Bioscience's MycoAlert detection kit. The cell line was validated using STR analysis as per WiCell certificate of analysis.

NC cell induction and terminal differentiation

Cranial hNC induction was performed according to Gomez et al. (2019). Terminal differentiation of hNC cells was performed by treating day 5 hNC cells with Accutase and plating cells into respective differentiation media on Matrigel-coated surfaces. Additional details can be found in the supplemental experimental procedures.

siRNA knockdown of ZEB2

ZEB2 siRNA knockdown was performed according to Prasad et al., 2020a using SMART Pool siRNA (Dharmacon L-006914-02) and NTC siRNA (Thermo Fisher Scientific AM4611). Knockdown efficiency was assessed using qRT-PCR and western blot analysis at NC day 2.

Generation of H1 ZEB2 N-terminal mutant line

Guide RNA (gRNA) sequences targeting ZEB2 exon 3 were designed using Synthego CRISPR Design Tool and cloned into the AAVS-T2 gRNA backbone (Mali et al., 2013) upstream of the gRNA scaffold sequence. We used a dual gRNA approach with gRNA target regions separated by 190 bp. gRNA sequences were as follows: GGTGAACT ATGACAATGTAG and GAATCTCGTTGTTGTGCCAG. To generate the mutant hESC line, H1 hESCs of passage 23 were nucleofected with gRNA plasmids and plasmid expressing hCas9 (Mali et al., 2013) using a Lonza 4D-Nucleofector. Transfected cells were cultured as single cells in CloneR (STEMCELL Technologies) and resulting colonies were expanded and screened using PCR followed by gel electrophoresis to visualize putative positive clones with ~200 bp deletions. Genotypes of putative homozygous mutant clones were determined by TA cloning (pGEM-T Easy Vector System; Promega) followed by Sanger sequencing to resolve compound heterozygous clones from true homozygotes. The mutant line reported is homozygous for a 199 bp deletion.

Gene expression analysis

Total RNA was extracted at indicated time points during hNC cell formation and terminal differentiation using TRIzol reagent and purified using the Direct-zol RNA kit (Zymo Research). For qRT-PCR analysis, 0.5–1 μg RNA was reverse transcribed using the PrimeScript RT Reagent Kit (Takara). qPCR was performed using SYBR Premix Ex Taq II (Takara) with a primer concentration of 300 nM. Primer sequences are listed in Table S5. Relative gene expression was calculated between the siRNA and NTC samples and normalized to the reference gene RPL13 using at least three biological replicates. For RNA-seq, RNA extracted from hNC cells was used with the NEBNext Poly(A) mRNA Magnetic Isolation Module (NEB) and the NEBNext Ultra II Directional RNA Library Prep Kit (NEB). RNA-seq experiments were performed in duplicate. Additional details can be found in the supplemental experimental procedures.

Chromatin accessibility and *de novo* motif analysis

ATAC-seq was performed on day 3 and day 5 hNC cells induced from the H1 N-terminal ZEB2 mutant and the isogenic WT line using the ATAC-Seq Kit from Active Motif with an input of 100,000 cells per reaction. Library quality was assessed using Agilent Bioanalyzer and libraries were sequenced on a NovaSeq6000. Additional details can be found in the supplemental experimental procedures. For *de novo* motif analysis, MEME was used with regions ±75 bp surrounding the peak center in differential enrichment mode. Peak sets representing up- and down-regulated peaks were analyzed independently with total peaks used as background. Putative binding proteins were identified using TOMTOM.

Chick *in situ* hybridization

Whole-mount chick *in situ* hybridization was performed as previously described (Basch et al., 2006). *ZEB2* antisense RNA probe was generated using T7 reverse transcriptase from template amplified from total chicken cDNA. Images were acquired using a SPOT SE camera and software using a Nikon Eclipse 80i microscope. Expression at each stage was assessed in at least 3 embryos, and a representative image is shown.

Protein analysis

Co-immunoprecipitation of ZEB2 and HDAC1 was performed by lysing day 5 hNC at 4°C for 1 h with rotation in lysis buffer (10 mM Tris-HCl [pH 7.4], 137 mM NaCl, 0.5% NP-40, and 1 mM EDTA) supplemented with protease inhibitor and PMSF, followed by centrifugation. ZEB2 was immunoprecipitated using 1.5 μg ZEB2 antibody (Santa Cruz Biotechnology) with overnight incubation at 4°C, followed by incubation with Dynabeads Protein G (Invitrogen) for 4 h. Protein was eluted in Lammeli buffer with β-mercaptoethanol. Immunoprecipitated and input protein was separated using SDS-PAGE followed by western blot analysis for HDAC1. HDAC1 was detected using HRP-conjugated secondary antibody, and the membrane subsequently stripped and probed for ZEB2. Western blotting to detect ZEB2 truncation was performed as previously described (Prasad et al., 2020a) using anti-ZEB2 and anti-GAPDH (Thermo Fisher Scientific).

Statistics

qRT-PCR graphs were generated and statistical analyses was performed using Prism. p values were determined using two-tailed unpaired t tests. RNA-seq and ATAC-seq were performed in duplicate, and 3 or more experiments were used for all others. RNA-seq differentially expressed genes were identified using DESeq2 (adjusted $p \leq 0.05$ and fold change ≥ 1.5). Differentially enriched ATAC-seq peaks were determined using Homer (fold-change cutoff of 2 and replicate false discovery rate [FDR] cutoff of 0.05).

SUPPLEMENTAL INFORMATION

Supplemental information can be found online at https://doi.org/10.1016/j.stemcr.2023.10.002.

ACKNOWLEDGMENTS

We thank Vincent Quiroz for help in generating the ZEB2 mutant line, Sujit Armstrong for bioinformatic assistance, the UCR Genomics Core, the UCR Stem Cell Core Facility, and the UCI Genomics High Throughput Facility. Some figures in this manuscript were created using images from Servier Medical Art (http://smart.servier.com), which are licensed under a Creative Commons Attribution 3.0 Unported License. This work was funded by NIH grants F32DE027862 and K99DE02978 to R.M.C. and NIH grant R01DE017914 to M.I.G.-C. M.S.P. is a recipient of a UC Riverside School of Medicine Dean's Postdoc to Faculty Fellowship.

AUTHOR CONTRIBUTIONS

Conceptualization, R.M.C. and M.I.G-C.; methodology, R.M.C. and M.S.P.; investigation, R.M.C., M.S.P., L.J.P., N.J.-S., and J.C.H.; data analysis, R.M.C. and J.W.; writing – original draft, R.M.C.; writing – review & editing, R.M.C., M.S.P., and M.I.G.-C.; funding acquisition, R.M.C. and M.I.G.-C.

DECLARATION OF INTERESTS

The authors declare no competing interests.

Received: November 21, 2021
Revised: September 30, 2023
Accepted: October 2, 2023
Published: October 26, 2023

REFERENCES

Acloque, H., Ocaña, O.H., Abad, D., Stern, C.D., and Nieto, M.A. (2017). Snail2 and Zeb2 repress P-cadherin to define embryonic territories in the chick embryo. Development *144*, 649–656.

Adam, M.P., Schelley, S., Gallagher, R., Brady, A.N., Barr, K., Blumberg, B., Shieh, J.T.C., Graham, J., Slavotinek, A., Martin, M., et al. (2006). Clinical features and management issues in Mowat–Wilson syndrome. Am. J. Med. Genet. *140*, 2730–2741.

Ahringer, J. (2000). NuRD and SIN3 histone deacetylase complexes in development. Trends Genet. *16*, 351–356.

Basch, M.L., Bronner-Fraser, M., and García-Castro, M.I. (2006). Specification of the neural crest occurs during gastrulation and requires Pax7. Nature *441*, 218–222.

Cacheux, V., Dastot-Le Moal, F., Kääriäinen, H., Bondurand, N., Rintala, R., Boissier, B., Wilson, M., Mowat, D., and Goossens, M. (2001). Loss-of-function mutations in SIP1 Smad interacting protein 1 result in a syndromic Hirschsprung disease. Hum. Mol. Genet. *10*, 1503–1510.

Charney, R.M., Prasad, M.S., and García-Castro, M.I. (2021). Diagnosis, Management and Modeling of Neurodevelopmental Disorders. In Diagnosis, Management and Modeling of Neurodevelopmental Disorders, C.R. Martin, V.R. Preedy, and R. Rajendram, eds., pp. 127–137.

Chng, Z., Teo, A., Pedersen, R.A., and Vallier, L. (2010). SIP1 Mediates Cell-Fate Decisions between Neuroectoderm and Mesendoderm in Human Pluripotent Stem Cells. Stem Cell *6*, 59–70.

Comijn, J., Berx, G., Vermassen, P., Verschueren, K., van Grunsven, L., van Roy, F., Bruyneel, E., Mareel, M., Huylebroeck, D., and Roy, F.V. (2001). The Two-Handed E Box Binding Zinc Finger Protein SIP1 Downregulates E-Cadherin and Induces Invasion. Mol. Cell *7*, 1267–1278.

DaSilva-Arnold, S.C., Kuo, C.-Y., Davra, V., Remache, Y., Kim, P.C.W., Fisher, J.P., Zamudio, S., Al-Khan, A., Birge, R.B., and Illsley, N.P. (2018). ZEB2, a master regulator of the epithelial–mesenchymal transition, mediates trophoblast differentiation. Mol. Hum. Reprod. *25*, 61–75.

Denecker, G., Vandamme, N., Akay, O., Koludrovic, D., Taminau, J., Lemeire, K., Gheldof, A., De Craene, B., Van Gele, M., Brochez, L., et al. (2014). Identification of a ZEB2-MITF-ZEB1 transcriptional network that controls melanogenesis and melanoma progression. Cell Death Differ. *21*, 1250–1261.

Douarin, N.L., and Kalcheim, C. (1999). The Neural Crest (Cambridge University Press).

Elloul, S., Elstrand, M.B., Nesland, J.M., Tropé, C.G., Kvalheim, G., Goldberg, I., Reich, R., and Davidson, B. (2005). Snail, Slug, and Smad-interacting protein 1 as novel parameters of disease aggressiveness in metastatic ovarian and breast carcinoma. Cancer *103*, 1631–1643.

Evans, E., Einfeld, S., Mowat, D., Taffe, J., Tonge, B., and Wilson, M. (2012). The behavioral phenotype of Mowat-Wilson syndrome. Am. J. Med. Genet. *158A*, 358–366.

Fardi, M., Alivand, M., Baradaran, B., Farshdousti Hagh, M., and Solali, S. (2019). The crucial role of ZEB2: From development to epithelial-to-mesenchymal transition and cancer complexity. J. Cell. Physiol. *234*, 14783–14799.

Gomez, G.A., Prasad, M.S., Sandhu, N., Shelar, P.B., Leung, A.W., and García-Castro, M.I. (2019). Human neural crest induction by temporal modulation of WNT activation. Dev. Biol. *449*, 99–106.

van Grunsven, L.A., Bellefroid, E.J., Papin, C., Avalosse, B., Opdecamp, K., Huylebroeck, D., Smith, J.C., and Bellefroid, E.J. (2000). XSIP1, a Xenopus zinc finger/homeodomain encoding gene highly expressed during early neural development. Mech. Dev. *94*, 189–193.

van Grunsven, L.A., Kricha, S., , et al.Taelman, V., Michiels, C., Verstappen, G., Souopgui, J., Nichane, M., Moens, E., Opdecamp, K., et al. (2007). XSip1 neuralizing activity involves the co-repressor CtBP and occurs through BMP dependent and independent mechanisms. Dev. Biol. *306*, 34–49.

Hackland, J.O.S., Shelar, P.B., Sandhu, N., Prasad, M.S., Charney, R.M., Gomez, G.A., Frith, T.J.R., and García-Castro, M.I. (2019). FGF Modulates the Axial Identity of Trunk hPSC-Derived Neural Crest but Not the Cranial-Trunk Decision. Stem Cell Rep. *12*, 920–933.

Heinritz, W., Zweier, C., Froster, U.G., Strenge, S., Kujat, A., Syrbe, S., Rauch, A., and Schuster, V. (2006). A missense mutation in the ZFHX1B gene associated with an atypical Mowat-Wilson syndrome phenotype. Am. J. Med. Genet. *140*, 1223–1227.

Imamichi, Y., König, A., Gress, T., and Menke, A. (2007). Collagen type I-induced Smad-interacting protein 1 expression downregulates E-cadherin in pancreatic cancer. Oncogene *26*, 2381–2385.

Ivanovski, I., Djuric, O., Caraffi, S.G., Santodirocco, D., Pollazzon, M., Rosato, S., Cordelli, D.M., Abdalla, E., Accorsi, P., Adam, M.P., et al. (2018). Phenotype and genotype of 87 patients with Mowat–Wilson syndrome and recommendations for care. Genet. Med. *20*, 965–975.

Kerosuo, L., and Bronner-Fraser, M. (2012). What is bad in cancer is good in the embryo: Importance of EMT in neural crest development. Semin. Cell Dev. Biol. *23*, 320–332.

LaBonne, C., and Bronner-Fraser, M. (1998). Neural crest induction in Xenopus: Evidence for a two-signal model. Development *125*, 2403–2414.

Lee, G., Chambers, S.M., Tomishima, M.J., and Studer, L. (2010). Derivation of neural crest cells from human pluripotent stem cells. Nat. Protoc. *5*, 688–701.

Leung, A.W., Murdoch, B., Salem, A.F., Prasad, M.S., Gomez, G.A., and García-Castro, M.I. (2016). WNT/β-catenin signaling mediates human neural crest induction via a pre-neural border intermediate. Development *143*, 398–410.

Mali, P., Yang, L., Esvelt, K.M., Aach, J., Guell, M., DiCarlo, J.E., Norville, J.E., and Church, G.M. (2013). RNA-Guided Human Genome Engineering via Cas9. Science *339*, 823–826.

Marchant, L., Linker, C., Ruiz, P., Guerrero, N., and Mayor, R. (1998). The inductive properties of mesoderm suggest that the neural crest cells are specified by a BMP gradient. Dev. Biol. *198*, 319–329.

Martin-Malpartida, P., Batet, M., Kaczmarska, Z., Freier, R., Gomes, T., Aragón, E., Zou, Y., Wang, Q., Xi, Q., Ruiz, L., et al. (2017). Structural basis for genome wide recognition of 5-bp GC motifs by SMAD transcription factors. Nat. Commun. *8*, 2070.

Menendez, L., Yatskievych, T.A., Antin, P.B., and Dalton, S. (2011). Wnt signaling and a Smad pathway blockade direct the differentiation of human pluripotent stem cells to multipotent neural crest cells. Proc. Natl. Acad. Sci. USA *108*, 19240–19245.

Mowat, D.R., Croaker, G.D., Cass, D.T., Kerr, B.A., Chaitow, J., Adès, L.C., Chia, N.L., and Wilson, M.J. (1998). Hirschsprung disease, microcephaly, mental retardation, and characteristic facial features: delineation of a new syndrome and identification of a locus at chromosome 2q22-q23. J. Med. Genet. *35*, 617–623.

Nitta, K.R., Tanegashima, K., Takahashi, S., and Asashima, M. (2004). XSIP1 is essential for early neural gene expression and neural differentiation by suppression of BMP signaling. Dev. Biol. *275*, 258–267.

Ohayon, D., Ventéo, S., Sonrier, C., Lafon, P.-A., Garcès, A., Valmier, J., Rivat, C., Topilko, P., Carroll, P., and Pattyn, A. (2015). Zeb Family Members and Boundary Cap Cells Underlie Developmental Plasticity of Sensory Nociceptive Neurons. Dev. Cell *33*, 343–350.

Postigo, A.A. (2003). Opposing functions of ZEB proteins in the regulation of the TGFbeta/BMP signaling pathway. EMBO J. *22*, 2443–2452.

Pradier, B., Jeub, M., Markert, A., Mauer, D., Tolksdorf, K., Van de Putte, T., Hrabě de Angelis, M., , et al.Seuntjens, E., Gailus-Durner, V., et al. (2013). Smad-interacting protein 1 affects acute and tonic, but not chronic pain. Eur. J. Pain *18*, 249–257.

Putte, T.V.D., Maruhashi, M., Francis, A., Nelles, L., Kondoh, H., Huylebroeck, D., and Higashi, Y. (2003). Mice lacking ZFHX1B, the gene that codes for Smad-interacting protein-1, reveal a role for multiple neural crest cell defects in the etiology of Hirschsprung disease-mental retardation syndrome. Am. J. Hum. Genet. *72*, 465–470.

Prasad, M.S., Charney, R.M., Patel, L.J., and García-Castro, M.I. (2020a). Distinct molecular profile and restricted stem cell potential defines the prospective human cranial neural crest from embryonic stem cell state. Stem Cell Res. *49*, 102086.

Prasad, M.S., Uribe-Querol, E., Marquez, J., Vadasz, S., Yardley, N., Shelar, P.B., Charney, R.M., and García-Castro, M.I. (2020b). Blastula stage specification of avian neural crest. Developmental Biology 458, 64–74.

Putte, T.V.D., Francis, A., Nelles, L., van Grunsven, L.A., and Huylebroeck, D. (2007). Neural crest-specific removal of Zfhx1b in mouse leads to a wide range of neurocristopathies reminiscent of Mowat-Wilson syndrome. Hum. Mol. Genet. *16*, 1423–1436.

Quintes, S., Brinkmann, B.G., Ebert, M., Fröb, F., Kungl, T., Arlt, F.A., Tarabykin, V., Huylebroeck, D., Meijer, D., Suter, U., et al. (2016). Zeb2 is essential for Schwann cell differentiation, myelination and nerve repair. Nat. Neurosci. *19*, 1050–1059.

Rogers, C.D., Saxena, A., and Bronner, M.E. (2013). Sip1 mediates an E-cadherin-to-N-cadherin switch during cranial neural crest EMT. J. Cell Biol. *203*, 835–847.

Rosivatz, E., Becker, I., Specht, K., Fricke, E., Luber, B., Busch, R., Höfler, H., and Becker, K.-F. (2002). Differential Expression of the Epithelial-Mesenchymal Transition Regulators Snail, SIP1, and Twist in Gastric Cancer. Am. J. Pathol. *161*, 1881–1891.

Rothstein, M., and Simoes-Costa, M. (2019). Heterodimerization of TFAP2 pioneer factors drives epigenomic remodeling during neural crest specification. Genome Res. *30*, 35–48.

Saint-Jeannet, J.-P., and Moody, S.A. (2014). Establishing the preplacodal region and breaking it into placodes with distinct identities. Dev. Biol. *389*, 13–27.

Seuntjens, E., Nityanandam, A., Miquelajauregui, A., Debruyn, J., Stryjewska, A., Goebbels, S., Nave, K.-A., Huylebroeck, D., and Tarabykin, V. (2009). Sip1 regulates sequential fate decisions by feedback signaling from postmitotic neurons to progenitors. Nat. Neurosci. *12*, 1373–1380.

Steventon, B., Araya, C., Linker, C., Kuriyama, S., and Mayor, R. (2009). Differential requirements of BMP and Wnt signalling during gastrulation and neurulation define two steps in neural crest induction. Development *136*, 771–779.

Stryjewska, A., Dries, R., Pieters, T., Verstappen, G., Conidi, A., Coddens, K., Francis, A., Umans, L., van IJcken, W.F.J., Berx, G., et al. (2016). Zeb2 Regulates Cell Fate at the Exit from Epiblast State in Mouse Embryonic Stem Cells. Stem Cell. *35*, 611–625.

Teraishi, M., Takaishi, M., Nakajima, K., Ikeda, M., Higashi, Y., Shimoda, S., Asada, Y., Hijikata, A., Ohara, O., Hiraki, Y., et al. (2017). Critical involvement of ZEB2 in collagen fibrillogenesis: the molecular similarity between Mowat-Wilson syndrome and Ehlers-Danlos syndrome. Sci. Rep. *7*, 46565.

van den Berghe, V., Stappers, E., Vandesande, B., Dimidschstein, J., Kroes, R., Francis, A., Conidi, A., Lesage, F., Dries, R., Cazzola, S., et al. (2013). Directed Migration of Cortical Interneurons Depends on the Cell-Autonomous Action of Sip1. Neuron *77*, 70–82.

Vandewalle, C., Comijn, J., De Craene, B., Vermassen, P., Bruyneel, E., Andersen, H., Tulchinsky, E., Van Roy, F., and Berx, G. (2005). SIP1/ZEB2 induces EMT by repressing genes of different epithelial cell-cell junctions. Nucleic Acids Res. *33*, 6566–6578.

Verschueren, K., Remacle, J.E., Collart, C., Kraft, H., Baker, B.S., Tylzanowski, P., Nelles, L., Wuytens, G., Su, M.T., Bodmer, R., et al. (1999). SIP1, a novel zinc finger/homeodomain repressor, interacts with Smad proteins and binds to 5′-CACCT sequences in candidate target genes. J. Biol. Chem. *274*, 20489–20498.

Verstappen, G., van Grunsven, L.A., Huylebroeck, D., Michiels, C., Van de Putte, T., Souopgui, J., Van Damme, J., Bellefroid, E., Vandekerckhove, J., and Huylebroeck, D. (2008). Atypical Mowat-Wilson patient confirms the importance of the novel association between ZFHX1B/SIP1 and NuRD corepressor complex. Hum. Mol. Genet. *17*, 1175–1183.

Wakamatsu, N., Yamada, Y., Yamada, K., Ono, T., Nomura, N., Taniguchi, H., Kitoh, H., Mutoh, N., Yamanaka, T., Mushiake, K., et al. (2001). Mutations in SIP1, encoding Smad interacting

protein-1, cause a form of Hirschsprung disease. Nat. Genet. *27*, 369–370.

Watt, K.E.N., and Trainor, P.A. (2013). Neurocristopathies - The Etiology and Pathogenesis of Disorders Arising from Defects in Neural Crest Cell Development, N. Crest Cells and P.A. Trainor, eds., pp. 361–394.

Wu, L.M.N., Wang, J., Conidi, A., Zhao, C., Wang, H., Ford, Z., Zhang, L., Zweier, C., Ayee, B.G., Maurel, P., et al. (2016). Zeb2 recruits HDAC–NuRD to inhibit Notch and controls Schwann cell differentiation and remyelination. Nat. Neurosci. *19*, 1060–1072.

Xia, M., Hu, M., Wang, J., Xu, Y., Chen, X., Ma, Y., and Su, L. (2010). Identification of the role of Smad interacting protein 1 (SIP1) in glioma. J. Neuro Oncol. *97*, 225–232.

Zweier, C., Horn, D., Kraus, C., and Rauch, A. (2006). Atypical ZFHX1B mutation associated with a mild Mowat-Wilson syndrome phenotype. Am. J. Med. Genet. *140*, 869–872.